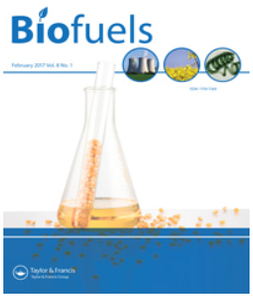

Biofuels

ISSN: 1759-7269 (Print) 1759-7277 (Online) Journal homepage: http://www.tandfonline.com/loi/tbfu20

Kinetic analysis of regional agro-industrial waste combustion

Anabel Fernandez, Alejandra Saffe, Germán Mazza & Rosa Rodriguez

To cite this article: Anabel Fernandez, Alejandra Saffe, Germán Mazza & Rosa Rodriguez (2017) Kinetic analysis of regional agro-industrial waste combustion, Biofuels, 8:1, 71-80, DOI: 10.1080/17597269.2016.1200865

To link to this article: http://dx.doi.org/10.1080/17597269.2016.1200865

BIOFUELS, 2017
VOL. 8, NO. 1, 71–80
http://dx.doi.org/10.1080/17597269.2016.1200865

Taylor & Francis
Taylor & Francis Group

Kinetic analysis of regional agro-industrial waste combustion

Anabel Fernandez[a], Alejandra Saffe[a], Germán Mazza[b] and Rosa Rodriguez[a]

[a]Instituto de Ing. Química, Fac. de Ingeniería, Univ. Nac. de San Juan, Libertador 1109 (O), San Juan, Argentina; [b]Instituto de Investigación y Desarrollo en Ingeniería de Procesos, Biotecnología y Energías Alternativas, CONICET-Universidad Nacional del Comahue, Neuquén, Argentina

ABSTRACT

Cuyo Region generates a significant quantity of agro-industrial wastes. To exploit this waste for energy production, a combustor was installed in this region. To improve its design and operation, a kinetic study of six agro-industrial wastes combustion, using thermogravimetric analysis, was made. The results show that this phenomenon occurs in four stages: drying, devolatilization, char combustion and residual combustion. Maximum weight loss occurs during the devolatilization stage, followed by the char combustion.

The contraction geometry's model describes the devolatilization, indicating that the degradation rate is controlled by the resulting reaction interface progress toward the solid center. Moreover, the first order reaction model describes the char combustion stages, showing that the reaction rate is proportional to remaining reactant(s) fraction. The highest energy activation values were obtained for sawdust at heating rate equal to 10 K/min and plum pits at heating rate equal to 15 K/min for devolatilization and char combustion, respectively, presenting slower reaction rate and more difficulty of a reaction starting.

For both analyzed stages, the activation energy values vary slightly with the heating rate. This variation can be due to the kinetic rate being controlled by the occurrence of physical transformation. It does not depend on mass but it depends on temperature.

ARTICLE HISTORY
Received 23 March 2016
Accepted 6 June 2016

KEYWORDS
Agro-industrial waste; combustion; kinetic model; thermogravimetric analysis

Introduction

Constant growth in mankind's energy requirements over the last century in addition to the high dependence on fossil fuels has resulted in important environmental challenges. In this scenario, renewable energy sources appear to be a sustainable tool to complement and gradually substitute fossil fuels in energy production. Among them, biomass, regarded as a feedstock for thermal conversion, presents some advantages such as its neutrality concerning CO_2 emissions during its life cycle [1] or its low N and S content that entails low NO_x and SO_2 emissions.[2]

Additionally, biomass is considered as an autonomous resource which partially avoids foreign energy dependence.[3] Because of the advantages when using biomass for energy production, it has experienced a huge surge in development in recent years. Nevertheless, it also presents some disadvantages, one of the most important being the generation of solid waste.[4]

In Cuyo Region, Argentina, one of the most important economic activities is the agro-industry, highlighting the wine, olive, wood and seasonal fruits industries such as peaches and plums. This sector produces a significant environmental impact in specific geographical areas. In this country, approximately 140,000 tons of peaches and plums are processed in the canning and jam industries, generating a solid biomass waste quantity of 79,800 tn/year. A quantity of marc and stalk equal to 51,928.3 tn/year is generated by the wine industry. About 150,000 tn/year of olive oil is produced, generating 70,000 tn/year of olive pits. Finally, the wood industry produces approximately 7000 tn/year of sawdust.[5] In order to exploit this waste to obtain energy, a combustor was installed in this region. Nevertheless, much of this potential is unused in spite of the environmental advantages and the economic benefits of this source of energy because some problems in current biomass combustion furnaces still exit. These problems, like low thermal efficiency, instability of heat load, and slagging, have to be improved to avoid the irrational use of biomass.

Thermographs elucidate the complexities in the thermal degradation of fuel substrates and their precursors. Consequently, the combustion kinetics can be deduced from the provided information by the thermographs for use in the design and control of combustion furnaces.

Kinetic parameters obtained in most of the studies are dependent not only on such factors such as atmosphere, sample mass, sample shape, flow rate, and heating rate, but also upon the mathematical treatment used to evaluate the data. The derivation of kinetic parameters including the activation energy and pre-exponential factor from the chemical reaction data has permeated much of the scientific literature.[6]

CONTACT Rosa Rodriguez rrodri@unsj.edu.ar

Various methods of kinetic analysis using different mathematical and methodological models have been discovered and developed. Generally, the kinetic parameters can be determined by three kinds of conventional methods [6] such as differential, integral, and maximum-reaction-rate ones that primarily originated by Friedman,[7] Coats and Redfern [8] and Kissinger.[9]

Knowledge of the chemical composition, the thermal behavior and the reactivity of these biomass fuels during combustion is very important for the effective design and operation of the thermochemical conversion units. Thermoanalytical techniques, in particular thermogravimetric analysis (TGA) and derivative thermogravimetry (DTG), allow us to obtain this information in a simple and straight forward manner. TGA is one of the commonly used techniques to study thermal events during the pyrolysis process of fuel.[10−15]

The combustion of waste biomass is a chemically complex process in which several reactions occur simultaneously. Because of this complexity, a large number of papers from the literature follow different approaches to describe the thermal degradation.[16−18]

Several kinetic equations for the description of solid-state reactions such as random nucleation, nucleation, geometry contraction and growth, diffusion and phase boundary controlled have been proposed and used during the last decades.[19]

Under oxidative atmosphere, the decomposition starts at a lower temperature and the degradation is faster than in an inert atmosphere. DTG curves of biomass combustion showed two separate peaks versus one peak in inert conditions: the first peak is attributed to simultaneous pyrolysis and oxidation of the raw material and the second peak logically to weight loss during oxidation of the char. Shen et al. [20] reported that the DTG curves were separated into two stages, with the first stage (low temperature region) in the range of 473−643 K and the second stage (high temperature region) in the range of 643−763 K. According to Branca and DiBlasi,[21] for the low temperature region, degradation characteristics were qualitatively similar to those observed in pure nitrogen. From a quantitative point of view, the presence of oxygen has been reported to predict and increase the devolatilization peaks: the DTG peaks were about 1.5 times higher than without oxygen. These results have been confirmed by other authors.[22,23]

In order to improve the combustor design and operation, the objective of this work is to study the kinetics of the oxidative decomposition of six agro-industrial wastes when heating at three different rates (5, 10 and 15 K/min) via thermogravimetrical measurements in an oxygen atmosphere to simulate combustion conditions. From the obtained thermogravimetric data, the kinetic parameters were calculated using the Coats−Redfern and Sharp isoconversional methods.

Materials and methods

Materials

This behavior during combustion of six lignocellulosic biomasses was studied: peach, plum and olive pits from canneries and jam industries, marc and stalk from wineries, and sawdust from the timber industry. All of these industries are located in the San Juan province, Argentina.

Proximate and ultimate analysis

Before the thermogravimetric analysis, the lignocellulosic biomass wastes were milled and sieved and the resulting 0.1−0.21 mm size fraction was used for the thermogravimetric tests. The weight loss at 378 K, ash and organic matter content were determined according to ASTM standards (ASTM D3173-87, ASTM D3172-89 (02)).[24,25] Elemental analysis of the samples was performed using elemental analyzer (EuroEA3000, EuroVector S.p.A., Germany). In order to calculate the high heating value, the correlation proposed by Channiwala and Parikh [26] was used (Table 1):

$$\mathrm{HHV}\ [\mathrm{MJ/kg}] = 0.3491\mathrm{C} + 1.1783\mathrm{H} + 0.1005\mathrm{S} - 0.1034\mathrm{O} - 0.0151\mathrm{N} - 0.0211\mathrm{A} \quad (1)$$

where C, H, S, O, N and A are the content of carbon, hydrogen, sulfur, oxygen, nitrogen and ash in the biomass (expressed as weight percentage), respectively.

Table 1. Ultimate and proximate analyses of six agro-industrial wastes.

	Peach pits	Stalk	Marc	Plum pits	Olive pits	Sawdust
Ultimate analysis						
C (%)	53.01	46.14	52.91	48.95	52.79	44.71
H (%)	5.90	5.74	5.93	1.38	2.57	1.48
N (%)	2.32	6.37	5.41	0.99	1.39	4.20
S (%)	1.88	4.21	5.34	0.27	0.50	0.28
O (%)*	36.89	37.54	30.41	48.41	42.75	49.33
Proximate analysis						
Ash (%, dry basis)	1.30	10.16	8.81	0.73	2.33	1.19
Volatile matter (%, total weight)	79.10	55.84	68.60	77.86	77.25	80.90
Fixed carbon (%, dry basis)	13.90	23.07	21.98	15.55	15.87	11.06
Weight loss at 378 K (%, total weight)	5.70	7.70	8.38	5.86	4.55	6.85
HHV (MJ/kg)	21.39	12.03	13.31	13.71	17.02	12.19

*By difference

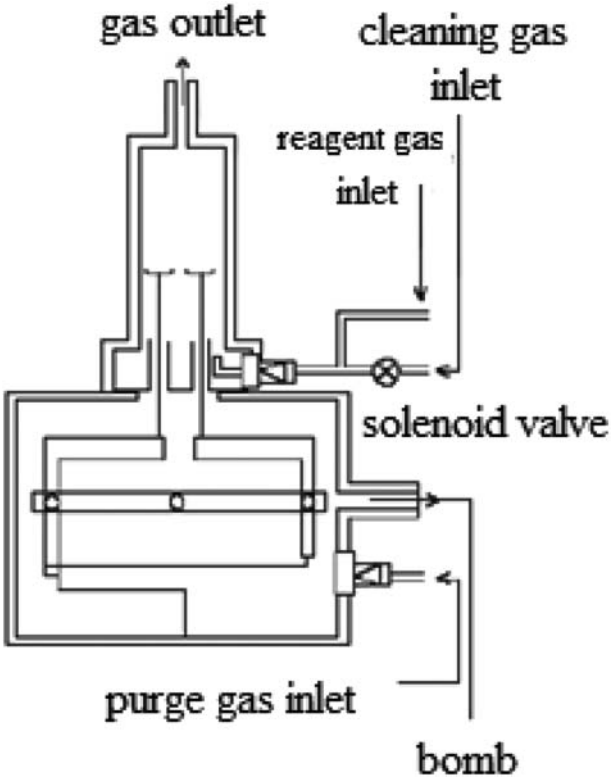

Figure 1. TGA equipment.

Methods

Thermogravimetric analysis

Thermogravimetric (TG) and DTG experiments of the powdered sample wastes were carried out using a microbalance (TGA-50, Shimadzu, North America), under oxidative atmosphere, heated from room temperature to 1173 K. A graphic of equipment usedis shown in the Figure 1 and its technical characteristics are given in Table 2. The experiments were performed at three different heating rates of 5, 10 and 15 K/min for each sample. To mitigate the difference of heat and mass transfer, all sample weights were kept at 12 mg approximately. In order to simulate the combustion, the composition of the atmosphere was 79% nitrogen and 21% oxygen. The flow rate was equal to 100 mL/min. The correction for TG data was done using a blank experiment. The reproducibility of the experiments was acceptable.

Kinetics analysis

Solid state kinetics can be studied with thermal methods by measuring the sample property as it is heated or held at a constant temperature. In this study, reaction kinetics was applied to thermal data obtained under non-isothermal conditions with a constant heating rate. The kinetics of biomass decomposition are routinely based on a single reaction and can be expressed by the following equation:

Table 2. Equipment used in thermogravimetric analysis.

Maximum temperature	1373 K
Balance type	TOP PLAN differential parallel guide
Heating rate	0.1 to 99.9 K/min
Minimum reading	0.001 mg
Measuring accuracy	±1%
Measurable range (TG)	±500 mg
Measurable range (DTA)	±1000 μv
Mass sample	1 g max.

$$-\frac{d\alpha}{dt} = K\, f(\alpha) \tag{2}$$

where t, α, $d\alpha/dt$, $f(\alpha)$ and K are time, conversion degree or extent of reaction, the process rate, conversion function and rate constant, respectively. The conversion function represents the reaction model used and depends on the controlling mechanism. The extent of reaction, α, can be defined as the mass fraction of biomass substrate that has decomposed and can be expressed as:

$$\alpha = \frac{mo - m}{mo - mf} \tag{3}$$

where m is the mass of the sample at a given time t; m_0 and m_f refer to values at the initial and final mass of samples remaining after the reaction, respectively.

K is the temperature function. The temperature dependence of the rate constant K for the process is described by the Arrhenius equation:

$$K = A\, e^{\frac{-E}{RT}} \tag{4}$$

where A is the pre-exponential factor, T is the absolute temperature, R is the universal gas constant and E is the apparent activation energy of the process. Substituting Equation (4) in Equation (2):

$$\frac{d\alpha}{dt} = A\, e^{\frac{-E}{RT}}\, f(\alpha) \tag{5}$$

If the temperature of the sample is changed by a controlled and constant heating rate, $\beta = dT/dt$, the variation in the conversion can be analyzed as a function of temperature, this temperature being dependent on the heating time. This variation can be expressed through a superficial transformation:

$$\frac{d\alpha}{dT} = \frac{d\alpha}{dt}\,\frac{dt}{dT} \tag{6}$$

where dt/dT describes the inverse of the heating rate in the case of nonisothermal conditions, $1/\beta$, $d\alpha/dt$ represents the isothermal reaction rate, and $d\alpha/dT$ denotes the nonisothermal reaction rate. An expression of the rate law for nonisothermal conditions can be obtained by substituting Equation (6)

in Equation (5):

$$\beta \frac{d\alpha}{dT} = A\, e^{\frac{-E}{RT}} f(\alpha) \quad (7)$$

where A (the pre-exponential factor) and E (the activation energy) are the Arrhenius parameters and R is the gas constant. Arrhenius parameters (A, E), together with the reaction model, f(α) are called the kinetic triplet. By separation of variable and integration, the following equation is obtained:

$$g(\alpha) = \int_0^{\alpha} \frac{d\alpha}{f(\alpha)} = {}^{A}/_{\beta} \int_{To}^{T} e^{-\frac{E}{RT}} dT \quad (8)$$

For nonisothermal conditions, there are several relationships used to compute Arrhenius parameters, each of which is based on an approximate form of the temperature integral.[27] Equation (8) can be rewritten by taking x = E/RT:

$$g(\alpha) = \int_0^{\alpha} \frac{d\alpha}{f(\alpha)} = \frac{AE}{\beta R} \int_o^{\infty} \frac{\exp(-x)}{x^2} dx = \frac{AE}{\beta R} .p(x) \quad (9)$$

where p(x) is the exponential integral.[27] Senum and Yang [27] developed an accurate nonlinear approximation of the temperature integral.

Several methods of performing kinetic analysis of solid state reactions are known. Generally, they can be grouped into: (1) Integral methods: If data used directly in weight loss versus temperature; (2) Differential methods: Using weight loss rate. The Coats−Redfern integral method is used more by the first group is based on the Arrhenius integral approximation. The Sharp differential method is used more by the second group and is based on reaction rate or its transformed mathematics.

The expression p(x) is expressed using the Coats−Redfern approximation:

$$p(x) = \frac{e^{-x}}{x^2} \quad (10)$$

Replacing p(x) in Equation (9) and applying logarithm to both members:

$$\ln \frac{g(\alpha)}{T^2} = \ln \frac{AR}{Ea\beta} - \frac{E}{RT} \quad (11)$$

Sharp [28] used the logarithm form of Equation (2):

$$\ln f(\alpha) = \frac{E}{RT} + \ln\left(\frac{d\alpha/dt}{A}\right) \quad (12)$$

The kinetic parameters are calculated following a similar method. Some of the more important rate equations used to describe the kinetic behavior of solid state reactions are listed in Table 3. These expressions are used to solve Equations (11) and (12).

Results and discussion

Characterization

Ultimate and proximate analyses of the six agro-industrial wastes are shown in Table 1. Considering the first analysis, the peach pits have the highest carbon (53.01%) content and the marc the highest hydrogen (5.93%) content. Stalk has the highest nitrogen (6.37%) content among the six materials. It is important to note that the biomass shows a higher O and H contents than the fossil fuels, producing smaller high heating values due to the smaller energy contained in C-O and C-H bonds than the C-C bonds.[29] The results shown in Table 1 are in agreement with those of other investigators: 48.30% C, 5.86% H, 0.21% N, 0% S and 45% O in sawdust reported by Biney et al. [30]; 49.87% C, 5.11% H, 1.38% N, 0.12% S and 42.07% O, in stalk reported by Valente et al. [31]; 46.88% C, 4.83% H, 0.93% N, 0.36%

Table 3. Expressions for the most common reaction mechanisms in solid state reactions.

Reaction model	f(α)	g(α)
Reaction order		
Zero order	$(1-\alpha)^n$	α
First order	$(1-\alpha)^n$	$-\ln(1-\alpha)$
nth order	$(1-\alpha)^n$	$(n-1)^{-1}(1-\alpha)^{1-n}$
Diffusional		
One dimensional diffusion	$1/(2\alpha)$	α^2
Two dimensional diffusion	$-1/\ln(1-\alpha)$	$(1-\alpha)\ln(1-\alpha)+\alpha$
Three dimensional diffusion (Jander)	$3(1-\alpha)^{2/3} / 2\,[1-(1-\alpha)^{1/3}]$	$[1-(1-\alpha)^{1/3}]^2$
Three dimensional diffusion (Ginstling-Brounstein)	$3/2\,[(1-\alpha)^{-1/3}-1]^{-1}$	$(1-2\alpha/3)-(1-\alpha)^{2/3}$
Nucleation		
Power law	$n(\alpha)^{(1-1/n)}$; n = 2/3, 1, 2, 3, 4	α^n n = 3/2, 1, 1/2, 1/3, 1/4
Exponential law	Ln (α)	α
Avrami-Erofeev	$n(1-\alpha)[-\ln(1-\alpha)]^{(1-1/n)}$; n = 1, 2, 3, 4	$[-\ln(1-\alpha)]^{(1/n)}$; n = 1, 2, 3, 4
Contracting geometry	$1/2\,\alpha$	
Contracting area	$(1-\alpha)^{(1-1/n)}$; n = 2	$(1-\alpha)^{(1/n)}$; n = 2
Contracting volume	$(1-\alpha)^{(1-1/n)}$; n = 3	$(1-\alpha)^{(1/n)}$; n = 3

S, and 41% O in cotton husk reported by Bhavanam et al.[32]

Taking into account the immediate analysis results, marc shows the highest weight loss at 378 K. It is necessary to consider that a high water content increases the energy requirements to carry out the thermal treatment, increases the residence time for drying and reduces the temperature, resulting in incomplete conversion of the hydrocarbons. These aspects decrease the process efficiency. Regarding the ash content of the agro-industrial wastes, a low percentage of it will minimize the production of fly and bottom ash and affect positively the high heating value (HHV).[26] Accordingly, plum pits show the smallest ash content, affecting positively its combustion process.

Demirbas and Arin [33] determined HHV for 16 different biomass fuels and reported similar values, Quirino et al. [34] reported similar values for wood. Peach pits show the highest HHV.

Concerning to the volatile contents, the obtained values (55.84−80.90 wt%) are comparative to the results reported by Jeguirim and Trouvé [35] (68.4 wt%) in arundo donax, Daouk et al. [36] (83.3 wt%, approximately) in pine wood and Crnkovic et al. [37] (79.7−98.6 wt%) in crude glycerin and beef tallow. Regarding fixed carbon, it was observed that the results of Jeguirim and Trouvé (18.4 wt%) and Daouk et al. (15.4 wt%, approximately) are similar to the obtained values in this work (11.06−23.07%, dry basis). The higher volatile matter/fixed carbon ratio improved the contact of reactants and reduced the residence time for the combustion process. Stalk shows the lowest value of this ratio.[38]

Thermogravimetric analysis

Thermogravimetric curves provide all information necessary to apply the kinetic models to oxidative degradation. Mass loss of all studied agro-industrial wastes with respect to the temperature during the TG analysis at heating rates of 5, 10 and 15 K/min are given in Figures 2, 3 and 4. TG and DTG curves (Figures 5, 6 and 7)

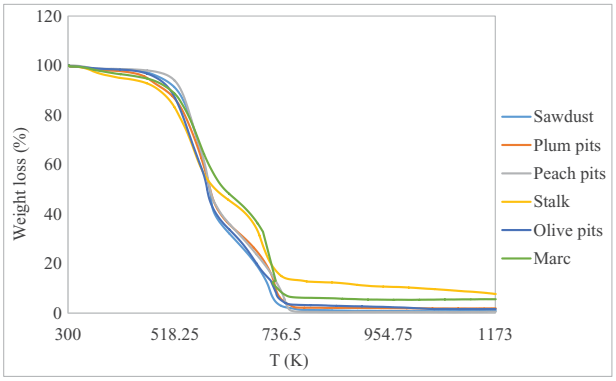

Figure 2. TG curves for the studied biomass samples at 5 K/min.

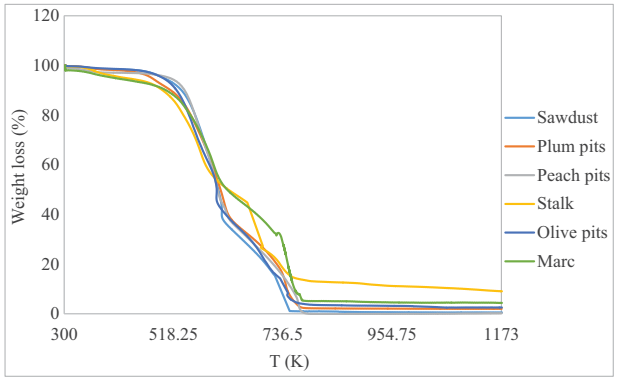

Figure 3. TG curves for the studied biomass samples at 10 K/min.

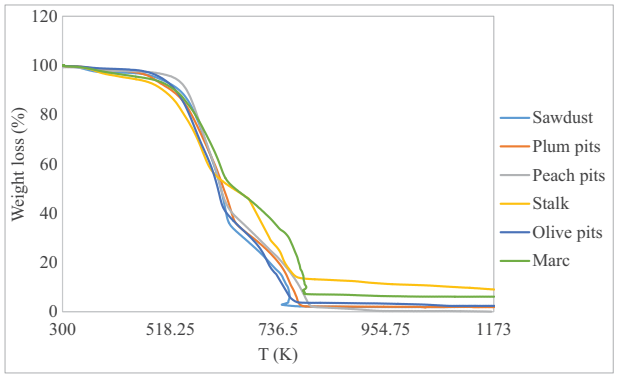

Figure 4. TG curves for the studied biomass samples at 15 K/min.

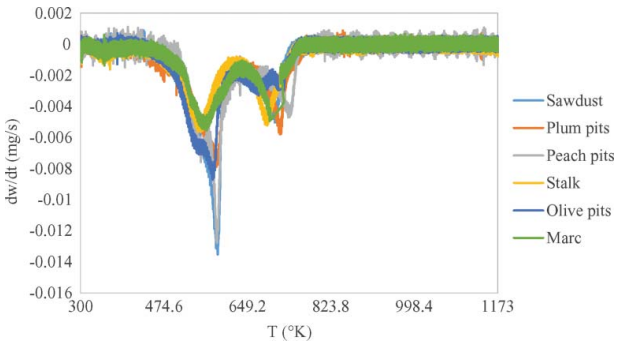

Figure 5. DTG curves for the studied biomass samples at 5 K/min.

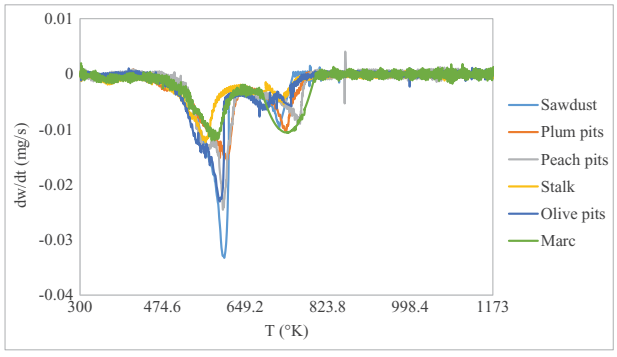

Figure 6. DTG curves for the studied biomass samples at 10 K/min.

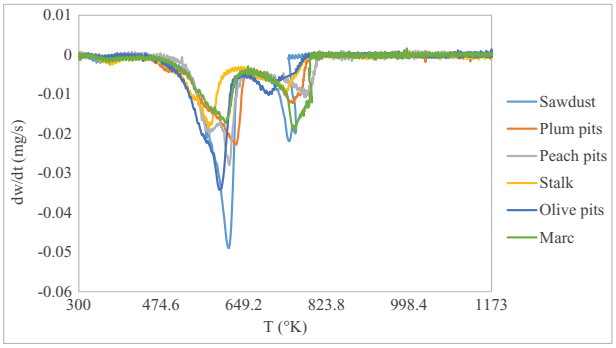

Figure 7. DTG curves for the studied biomass samples at 15 K/min.

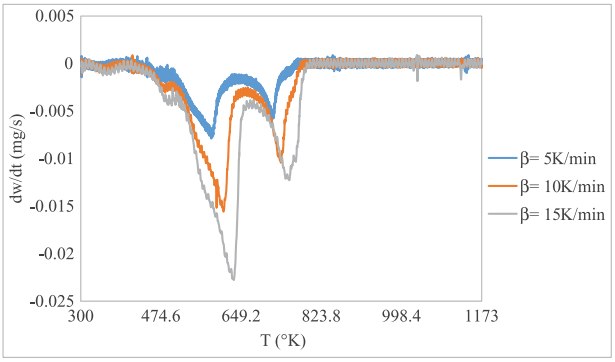

Figure 8. Comparison of the weight loss rates for plum pits.

show the physical and chemical structural changes occurring during thermal conversion. Four stages of oxidative decomposition can be observed in these curves: (a) drying and light volatile release (T < 473 K), (b) devolatilization (473 K < T < 623 K), (c) char combustion (623 K < T < 773 K) and (d) residual combustion (773 K < T < 1173 K). These stages are associated with the peaks in the DTG curves and thus with the changes of the slopes of the TG curves. The analyzed wastes show small differences regarding temperature ranges. The initial and last temperatures of different stages for the six biomasses are different from each other. The differences for all agro-industrial wastes samples can be attributed to variations of hemicellulose, lignin and cellulose contents.[39]

Most weight loss occurs in the devolatilization stage, giving average values equal to 56, 55, 54, 42, 45 and 43% for peach pits, olive pits, plum pits, stalk, marc and sawdust, respectively. Comparing the weight loss rate for the studied wastes during this stage, the sawdust showed the highest value of this parameter at all heating rates, and marc the lowest value. The temperature for the maximum decomposition rate in this stage depends on the agro-industrial waste composition.

Another step in which high weight loss occurs is the char combustion: 25, 29, 27, 31, 38, and 23% for peach pits, olive pits, plum pits, stalk, marc and sawdust, respectively (average values).

At temperatures higher than 773 K, almost no weight loss was observed. When the temperature increases during heat-up, the evolution of different products or groups of products occurs in segmented (but overlapping) phases. During the first stage (T < 393 K), the moisture evolution is produced, then (393 K < T < 723 K) gases release occurs, primarily CO_2 and CH_4, and later (723 K < T < 873 K) the release of chemically bonded CO_2 and chemically formed H_2O.[33] At temperatures higher than 873 K, species such as carbon oxides, tars and hydrocarbon gases (heavy hydrocarbons such as fluorene, phenanthrene, fluoranthene, and benzo (a) pyrene) were identified in the gas phase. At higher temperatures, carbon oxides are the primary products.[40]

The obtained curves have the typical appearance of degradation of lignocellulosic biomass. Cellulose, hemicellulose and lignin are the main components of lignocellulosic biomass.[41] The thermal stability of three components are hemicellulose < cellulose < lignin. Hemicellulose degradation begins about 453 K and ends about 623 K. Cellulose is comparatively stable, hemicellulose is decomposed in the following temperature range: 473−648 K. Lignin has a different behavior, the decomposition initiation temperature is similar to hemicellulose, but its decomposition process lasts until the heating program ends and the mass loss rate is almost constant during the reaction.[42]

Figure 8 demonstrates an example of a set of DTG curves (plum pits), obtained at 5 K/min, 10 K/min and 15 K/min heating rates in an air atmosphere. It can be observed that there is a shift in the weight loss curves caused by various heating rates. At higher heating rates, the weight loss rate is higher too. The maximum weight loss rate of different agro-industrial wastes for devolatilization stage reached at 546−586 K at a heating rate of 5 K/min; it is 565−612 K and 580−633 K at 10 and 15 K/min. The combustion char stage reached at 681−738 K at a heating rate of 5 K/min; it is 691−765 K and 707−779 K at 10 and 15 K/min.

This is related to the heat transfer limitation. At higher heating rates, this limitation is higher because stronger thermal shock is being acquired over a short time and there is greater temperature gradient between the inside and outside; this aspect does not favor the release of volatile matter.[43]

Kinetic model

The kinetic models proposed in this study describe the devolatilization and the char combustion stages because, during these phenomena, the maximum weight loss is produced. These processes have mechanisms very often unknown or too complex to be characterized by a simple kinetic model. They generally occur in multiple steps and, in order to describe their kinetics, isoconversional methods are often used.[44] These methods have the ability to reveal the

complexity of the process in the form of a functional dependence of the activation energy on the extent of conversion. Application of a model-free method was recommended in order to obtain a reliable kinetic description of the investigated process. The basic assumption of these models is that the reaction rate for a constant extent of conversion depends only on the temperature.

The fitting of the experimental data of g (α) and f (α) versus temperature to all proposed models (Table 3) was performed by means of the Marquardt-Levenberg [45] algorithm, using Data Fit 9.1 software. In order to estimate the E and A parameters, least squares nonlinear regression was used. With the purpose of evaluating each model, an estimation of the parameter values is needed. The statistical parameters determined apart from the determination coefficient, R^2, were the reduced chi-square, χ^2, defined by:

$$\chi^2 = \frac{\Sigma_1^N \left(X_{exp,\,i} - X_{pre,i}\right)^2}{N - z} \tag{12}$$

where $X_{exp,i}$ is the experimental value, $X_{pre,i}$ is the predicted value, N is the number of experimental data points, and z is the number of parameters in the model.

The highest R^2 values and the smallest χ^2 values are presented for the devolatilization stage, the contraction geometry's model, and for the char combustion, the first order reaction model. These models are applied for all agro-industrial wastes using the integral Coats−Redfern method.

The contraction geometry's model describes the devolatilization stage characteristics under oxidative atmosphere for all biomass wastes obtained by nonisothermal TGA and it assumes that nucleation occurs rapidly on the surface of the crystal. The rate of degradation is controlled by the resulting reaction interface progress toward the center of the solid.[46]

Order-based models are the simplest models as they are similar to those used in homogeneous kinetics. In these models, the reaction rate is proportional to amount or fraction remaining of reactant(s) raised to a particular power (integral or fractional) which is the reaction order.

It is important to note that the best results were obtained using the Coats−Redfern method, due to the numerical differentiation of experimental data being highly susceptive to data noise [47] which can result in significant scatter in the resulting derivative curves. Widespread use of the Sharp method has also been inhibited because of the daunting calculations.[48]

In order to calculate the activation energy and pre-exponential factor, the contracting volume, first order reaction models (for the devolatilization and the char combustion steps, respectively) and the Coats−Redfern method were used. Table 4 shows the obtained kinetic parameters and the statistical parameters values for different studied agro-industrial wastes in the devolatilization stage. Table 5 shows the same parameters for the char combustion stage. For the first model, the R^2 and χ^2 values were between 0.98−0.99 and $1.15^{*}10^{-4}$ and $1.33^{*}10^{-3}$, respectively. For the second model, the R^2 and χ^2 values were between 0.97−0.99 and $1.15^{*}10^{-14}$ and $3.23^{*}10^{-13}$, respectively. The higher values of R^2 and the lower values of χ^2, the better is the goodness of fit. Figures 9 and 10 show the comparison of experimental data and the predicted values for peach pits at different heating rates during both studied stages.

The obtained values of activation energy vary between 68.89 and 114.36 kJ/mol and 74.94 and 195.36 kJ/mol for the devolatilization and char combustion stage respectively for all studied agro-industrial wastes. The calculated values of E vary slightly with the heating rate. The increasing of heating rate leads to a simultaneous increase of the heat effect. [49,50] Increasing the heating rate signifies that a higher temperature is required to set off the oxidative pyrolysis process. The highest value of the energy activation for the devolatilization stage was predicted for sawdust at a heating rate equal to 10 K/min and the smallest value of this parameter was calculated for stalk at 5 K/min. The highest value of the energy activation for the char combustion stage was predicted for plum pits at a heating rate equal to 15 K/min and the smallest value of this parameter was calculated for sawdust at 15 K/min. Activation energy represents the minimum energy requirement for a reaction to get started, in other words, a higher value of activation energy means slower reaction rate and more difficulty of a reaction starting. The found activation energy values are similar to obtained values by Shanchao et al. [51] The calculated values of pre-exponential factor were between $8.68^{*}10^{9}$ and $2.08^{*}10^{14}s^{-1}$ and between $5.82^{*}10^{5}$ and $1.45^{*}10^{13}s^{-1}$ for the devolatilization and char combustion stage, respectively. This parameter also augments with the heating rate increase.

Figure 11 shows the plots of ln (β/T^2) vs. 1/T for the several conversion degrees (α) corresponding to the plum pits during the char combustion stage. The coefficient of correlation (R^2) for all the lines drawn at various conversions (0.1−0.7) is greater than 0.97, which indicates the best fit. The activation energy is constant at different heating rates. However, for the olive pits, this coefficient of correlation is 0.94, indicating that the energy activation values may be different. This also implies the possibility of a simultaneous reaction mechanism.

Conclusions

In order to improve the design and operation of the combustor, a kinetic study of six regional

Table 4. Pre-exponential factor and activation energy obtained and statistical parameter values in the devolatilization stage.

	Heating rate	Temperature range	Temperature peak	Mass loss rate maximum	Kinetics parameters		Statistical parameters	
Agro-industrial wastes	β (K/min)	(K)	(K)	(mg/s)	E (kJ/mol)	A (s^{-1})	R^2	χ^2
Sawdust	5	517 604	586	0.013	84.83	$5.63*10^{11}$	0.98	$1.07*10^{-3}$
	10	526 615	601	0.032	114.36	$2.08*10^{14}$	0.98	$1.04*10^{-3}$
	15	534 634	618	0.049	109.38	$6.47*10^{13}$	0.98	$4.29*10^{-4}$
Plum pits	5	503 628	584	0.008	84.81	$5.43*10^{11}$	0.99	$4.28*10^{-4}$
	10	506 636	612	0.015	103.27	$1.94*10^{13}$	0.98	$6.70*10^{-4}$
	15	512 652	633	0.023	98.22	$6.82*10^{12}$	0.99	$4.58*10^{-4}$
Peach pits	5	509 610	585	0.013	81.17	$2.61*10^{11}$	0.99	$7.09*10^{-4}$
	10	519 632	603	0.024	99.83	$2.12*10^{13}$	0.99	$2.33*10^{-4}$
	15	525 646	618	0.028	107.13	$8.43*10^{13}$	0.99	$4.94*10^{-4}$
Stalk	5	461 607	552	0.006	64.89	$8.68*10^{9}$	0.98	$1.19*10^{-3}$
	10	477 603	565	0.012	71.86	$3.75*10^{10}$	0.98	$1.06*10^{-3}$
	15	488 617	580	0.018	80.69	$2.26*10^{11}$	0.99	$4.89*10^{-4}$
Olive pits	5	487 609	577	0.009	74.73	$6.84*10^{10}$	0.99	$7.04*10^{-4}$
	10	505 607	598	0.023	96.51	$5.92*10^{12}$	0.98	$9.27*10^{-4}$
	15	494 629	600	0.034	103.50	$4.12*10^{13}$	0.98	$1.33*10^{-3}$
Marc	5	488 631	561	0.005	77.75	$1.23*10^{11}$	0.99	$4.78*10^{-4}$
	10	501 632	587	0.012	97.89	$7.43*10^{12}$	0.99	$1.15*10^{-4}$
	15	498 642	610	0.017	102.73	$1.69*10^{13}$	0.98	$6.07*10^{-4}$

Table 5. Pre-exponential factor and activation energy obtained and statistical parameter values in the char combustion stage.

	Heating rate	Temperature range	Temperature peak	Mass loss rate maximum	Kinetics parameters		Statistical parameters	
Agro-industrial wastes	β (K/min)	(K)	(K)	(mg/s)	E (kJ/mol)	A (s^{-1})	R^2	χ^2
Sawdust	5	662 744	708	0.005	93.45	$1.14*10^{6}$	0.98	$1.99*10^{-13}$
	10	687 750	720	0.009	88.37	$5.82*10^{5}$	0.98	$1.15*10^{-14}$
	15	689 479	744	0.022	74.94	$7.60*10^{7}$	0.99	$1.24*10^{-14}$
Plum pits	5	667 760	719	0.006	146.01	$7.41*10^{9}$	0.99	$3.23*10^{-13}$
	10	686 790	737	0.010	186.93	$6.65*10^{12}$	0.99	$1.19*10^{-14}$
	15	699 796	748	0.012	195.36	$1.67*10^{13}$	0.99	$3.08*10^{-14}$
Peach pits	5	678 764	738	0.005	192.35	$1.45*10^{13}$	0.99	$1.15*10^{-13}$
	10	714 785	765	0.009	174.85	$5.91*10^{11}$	0.96	$7.95*10^{-14}$
	15	733 813	779	0.011	143.87	$6.39*10^{9}$	0.98	$3.44*10^{-14}$
Stalk	5	649 760	694	0.005	106.22	$1.15*10^{7}$	0.99	$5.97*10^{-14}$
	10	655 759	729	0.005	103.45	$1.03*10^{7}$	0.98	$1.47*10^{-13}$
	15	665 787	742	0.009	161.31	$1.78*10^{11}$	0.98	$1.52*10^{-13}$
Olive pits	5	637 752	681	0.003	106.93	$1.25*10^{7}$	0.98	$2.17*10^{-13}$
	10	653 772	691	0.006	170.42	$6.31*10^{11}$	0.98	$1.35*10^{-13}$
	15	672 784	707	0.010	174.01	$1.38*10^{12}$	0.98	$1.55*10^{-13}$
Marc	5	656 750	697	0.005	148.31	$9.55*10^{9}$	0.99	$8.66*10^{-14}$
	10	687 798	725	0.010	187.38	$5.63*10^{12}$	0.97	$9.79*10^{-14}$
	15	683 795	759	0.020	118.81	$3.63*10^{7}$	0.99	$3.09*10^{-14}$

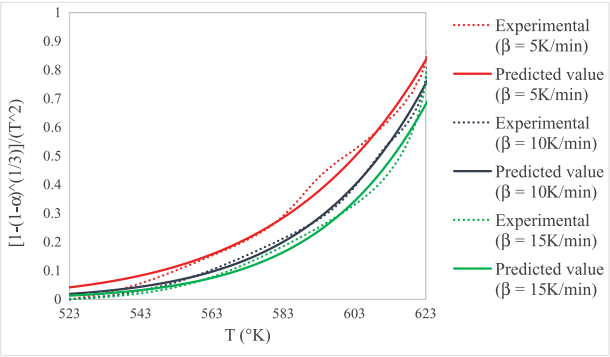

Figure 9. Comparison of experimental and predicted values of g (α) for peach pits under an oxidative atmosphere in the devolatilization stage at different heating rates.

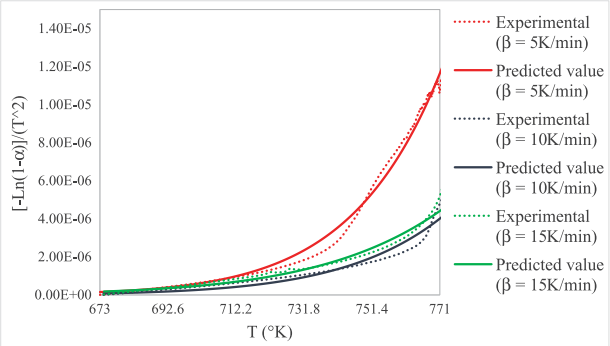

Figure 10. Comparison of experimental and predicted values of g (α) for peach pits under an oxidative atmosphere in the char combustion stage at different heating rates.

lignocellulosic wastes (sawdust, marc, stalks, and peach, plum and olive pits) was carried out using TGA analysis. The following conclusions are obtained:

- Peach pits show the highest C content and HHV.
- The moisture content of all studied agro-industrial wastes is smaller than 8.38%, indicating that the energy for their drying is low.
- Plum pits show the smallest ash content, minimizing the production of fly and bottom ash during its combustion.

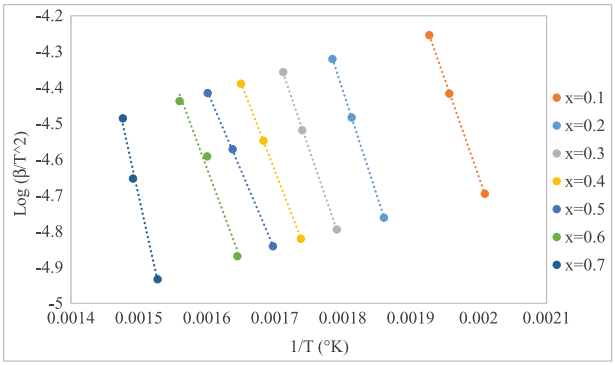

Figure 11. Typical Coats–Redfern plot of plum pits.

- TG and DTG curves show that the combustion process occurs in four stages: drying, devolatilization, combustion char and residual combustion.
- The contraction geometry's model describes the devolatilization stage. The highest value of the energy activation was obtained for sawdust at a heating rate equal to 10 K/min, presenting slower reaction rate and more difficulty of a reaction starting.
- The first order reaction model describes the char combustion step. The highest value of the energy activation was predicted for plum pits at a heating rate equal to 15 K/min.
- For both analyzed stages, the obtained values of activation energy vary slightly with the heating rate for all studied agro-industrial wastes. This variation can be due to the kinetic rate of these stages is controlled by the physical transformation caused by the temperature, which does not depend on the mass.

Disclosure statement

No potential conflict of interest was reported by the authors.

References

[1] Fouilland T, Grace J, Ellis N. Recent advances in fluidized bed technology in biomass processes. Biofuels. 2010;3 (1):409–433
[2] Kenney KL, Smith WA, Gresham GL, et al. Understanding biomass feedstock variability. Biofuels. 2013;1(4): 111–127.
[3] Demirbas A. Importance of biomass energy sources for Turkey. Energ Policy. 2008;36:834–42.
[4] Sebastián F, García D, Rezeau A. Energía de la biomasa. (Serie Energías renovables). Vol. 1. España: Prensas Universitarias de Zaragoza. 2010. ISBN 978-84-92774-91-3.
[5] Informe Técnicos. Buenos Aires: Instituto Nacional de Tecnología Agropecuaria. 2015 ISSN 22508481.
[6] Burnham AK, Braun RL. Global kinetic analysis of complex materials. Energy Fuels. 1999;13:1–22.
[7] Friedman HL. Kinetics of thermal degradation of char-forming plastics from thermogravimetry. Application to a phenolic plastic. Journal of Polymer Science Part C: Polymer Symposia. 1964;6(1):183–195.
[8] Coats AW, Redfern JP. Kinetic parameters from thermogravimetric data. Nature. 1964;201:68–69.
[9] Kissinger H. Reaction Kinetic in differential thermal analysis. Anal Chem. 1957;29:1702.
[10] Kök MV, Pamir R. Pyrolysis kinetics of oil shales determined by DSC and TG/DTG. Oil Shale. 2003;20:57–68.
[11] Kök MV. Coal pyrolysis: thermogravimetric study and kinetic analysis. Energ Sources. 2003;25:1007–1014.
[12] Kök MV, Karacan O. Pyrolysis analysis and kinetics of crude oils. J. Therm. Anal. Calorim. 1998;52:781–788.
[13] Borah D, Barua M, Baruah MK. Dependence of pyrite concentration on kinetics and thermodynamics of coal pyrolysis in non-isothermal systems. Fuel Process. Technology. 2005;86:977–993.
[14] Aouad A, Bilali L, Benchanâa M, et al. Kinetic aspect of thermal decomposition of natural phosphate and its

kerogen. Influence of heating rate and mineral matter. J. Therm. Anal. Calorim. 2002;67:733−743.
[15] Kök MV. Temperature-controlled combustion and kinetics of different rank coal samples. J. Therm. Anal. Calorim. 1998;79:175−180.
[16] Jankovi B, Kolar-Aníc L, Smičiklas I, et al. The non-isothermal thermogravimetric tests of animal bones combustion. Part. I. Kinetic analysis. Thermochimica Acta. 2009;495:129−138.
[17] Fuying M, Yelin Z, Jinjin W, et al. Thermogravimetric study and kinetic analysis of fungal pretreated corn stover using the distributed activation energy model. Bioresource Technol. 2013;128:417−422.
[18] Huang YF, Kuan WH, Chiueh PT, et al. A sequential method to analyze the kinetics of biomass pyrolysis. Bioresource Technol. 2011;102:9241−9246.
[19] Brown ME, Dollimore D, Galwey AK. Reactions in the Solid State. Amsterdam, The Netherlands: Elsevier Scientific Publishing; 1980.
[20] Shen DK, Gu S, Luo KH, et al. Kinetic study on thermal decomposition of Woods in oxidative environment. Fuel. 2009;88:1024−1030.
[21] Branca C, DiBlasi C. Global interinsic kinetics of Wood oxidation. Fuel. 2004;83:81−87.
[22] Amutio M, Lopez G, Aguado R, et al. Kinetic study of lignocellulosic biomass oxidative pyrolysis. Fuel. 2012; 95:305−311.
[23] Su Y, Luo Y, Wu W, et al. Characteristics of pine Wood oxidative pyrolysis: degradation behavior, carbón oxide production and heat properties. J. Anal. Appl. Pyrolysis. 2012;98:137−143.
[24] ASTM D3173 − 87. Standard Test Method for Moisture in the Analysis Sample of Coal and Coke. West Conshohocken (PA): Standards & Publications; 1996.
[25] ASTM D3172 − 89. Standard Practice for Proximate Analysis of Coal and Coke. West Conshohocken (PA): Standards & Publications; 2002.
[26] Channiwala SA, Parikh APP. Unified correlation for estimating HHV of solid, liquid and gaseous fuels. Fuel. 2002;81(8):1051−1063.
[27] Senum GI, Yang RT. Rational approximations of the integral of the Arrhenius function. J Therm Anal. 1977;11:445−447.
[28] Sharp JH, Achar BNN. Proceeding of the International Clay Conference. 1966;1:1−67.
[29] Van Krevelen DW. Coal typology physics chemistry constitution. 3rd ed. Amsterdam: Elsevier; 1993.
[30] Biney P, Gyamerah M, Shen J, et al. Kinetics of the pyrolysis of arundo, sawdust, corn stover and switch grass biomass by thermogravimetric analysis using a multistage model. Bioresource Technol. 2015;179:113−122.
[31] Valente M, Brillard A, Schönnenbeck C, et al. Investigation of grape marc combustion using thermogravimetric analysis. Kinetic modeling using an extended independent parallel reaction (EIPR). Fuel Process Technol. 2015;131:297−303.
[32] Bhavanam A, Sastry RC. Kinetic study of solid waste pyrolysis using distributed activation energy Model. Bioresource Technol. 2014;178:126−131.
[33] Demirbas A, Arin G. An overview of biomass pyrolysis. Energ Sources. 2002;24(5):471−482.
[34] Quirino W, Vale A, Andrade A, et al. Poder calorífico da madeira e de materiais lignocelulósicos. Revista da Madeira. 2005;89:100−106.
[35] Jeguirim M, Trouvé G. Pyrolysis characteristics and kinetics of Arundo donax using thermogravimetric analysis. Bioresource Technol. 2009;100:4026−4031.
[36] Daouk E, Van de Steene L, Paviet F, et al. Thick wood particle pyrolysis in an oxidative atmosphere. Chem Eng Sci. 2015;126:608−615.
[37] Crnkovic PM, Koch C, Ávila I, et al. Determination of the activation energies of beef tallow and crude glycerin combustion using thermogravimetry. Biomass and Bioenergy. 2012;44:8−16.
[38] Obernberger I, Thek G. Physical characterisation and chemical composition of densified biomass fuels with regard to their combustion behaviour. Biomass and Bioenergy. 2004;27:653−69.
[39] Yang H, Yan R, Chen H, et al. Characteristics of hemicellulose, cellulose and lignin pyrolysis. Fuel. 2007;86: 1781−1788, I. 12−13.
[40] Zheng G, Kozi JA. Thermal events occurring during the combustion of biomass residue. Fuel. 2000;79:181.
[41] Burnham A, Dinh L. A comparison of isoconversional and model-fitting approaches to kinetic parameter estimation and application predictions. J Therm Anal Calorim. 2007;89:479−490.
[42] Su Y, Luo Y, Wu WG, et al. Characteristics of pine wood oxidative pyrolysis: Degradation behavior, carbón oxide production and heat properties. J Anal Appl Pyrol. 2012;98:137−143.
[43] Wang L, Hustad JE, Skreiberg Ø, et al. A critical review on additives to reduce ash related operation problems in biomass combustion applications. Energy Procedia. 2012;20:20−29.
[44] Chouchene A, Jeguirim M, Khiari B, et al. Thermal degradation of olive solid waste: Influence of particle size and oxygen Concentration. Resources, Conservation and Recycling. 2010;54:271−277.
[45] DataFit 9.1, trial version. Available from: http://www.oakdaleengr.com/download.htm on May 20, by Siyu Chen 2008.
[46] Jacobs PWM, Tompkins FC. Classification and theory of solid reactions. In Chemistry of the solid state; Garner, WE, editor. New York: Academic Press; Chapter 7; 1955.
[47] Cai J, Liu R, Sun C. Logistic regression model for isoconversional kinetic analysis of cellulose pyrolysis. Energ Fuels. 2008;22:867−870.
[48] Flynn JH. A general differential technique for the determination of parameters: energy of activation, preexponential factor and order of reaction (when applicable). J Therm Anal. 1991;37:293−305.
[49] Amutio M, Lopez G, Aguado R, et al. Kinetic study of lignocellulosic biomass oxidative pyrolysis. Fuel. 2012;95: 305−311.
[50] Sanchez Silva L, Lopez Gonzalez D, Garcia Minguillan AM, et al. Pyrolysis, combustion and gasification characteristics of Nannochloropsis gaditana microalgae. Bioresource Technol. 2013;130:321−331.
[51] Shanchao Hu, Xiaoqian Ma, Yousheng Lin, et al. Thermogravimetric analysis of the co-combustion of paper mill sludge and municipal solid waste. Energ Convers Manage. 2015;99:112−118.